RSC Advances

PAPER

View Article Online
View Journal | View Issue

Cite this: *RSC Adv.*, 2020, **10**, 31470

Effect of lemon peel flavonoids on UVB-induced skin damage in mice

Jun Wang,[ab] Yunfeng Bian,[c] Yujiao Cheng,[ab] Rongrong Sun[ab] and Guijie Li *[abd]

By establishing an effective ultraviolet B (UVB) radiation model of skin damage in mice, the effect of lemon peel flavonoids (LPF) on skin damage was explored. UVB skin damage in UV-irradiated mice was simulated, and animal models were established. Serum parameters were measured using kits, skin sections were stained with hematoxylin–eosin (H&E) and Masson, and quantitative polymerase chain reaction (qPCR) was used to detect the expression of skin tissue-related mRNA. The experimental results showed that LPF increased the activity of catalase (CAT) and superoxide dismutase (SOD) oxidases in serum of mice with UVB-induced skin damage and decreased MDA, interleukin-1β (IL-1β), IL-6, IL-10, and tumor necrosis factor-alpha (TNF-α) levels. Pathological observation indicated that LPF alleviated the skin tissue lesions caused by UVB. LPF upregulated the mRNA expression of *SOD1*, *SOD2*, *CAT*, nuclear factor erythroid-2 related factor 2 (*Nrf2*), heme oxygenase-1 (*HO-1*), and inhibitor of NF-κB alpha (*IκB-α*) and downregulated the expression of nuclear factor kappa B (*NF-κB*), *p38 MAPK*, and cyclooxygenase-2 (*COX-2*) in the skin tissue of skin-damaged mice. There was a greater protective effect of LPF on the skin as compared to vitamin C (VC) at the same application concentration, and the effect of LPF was positively correlated with the concentration. High performance liquid chromatography (HPLC) analysis showed that LPF contained five flavonoid compounds, namely isomangiferin, rutin, astragalin, naringin, and quercetin. We demonstrated that flavonoids from LPF exhibit an excellent skin protection effect with satisfactory application value.

Received 23rd June 2020
Accepted 10th August 2020

DOI: 10.1039/d0ra05518b

rsc.li/rsc-advances

1 Introduction

In practical applications, ultraviolet (UV) radiation is distinguished according to wavelength, which can be specifically divided into short-wave UVC (200–280 nm), medium-wave UVB (280–320 nm), and long-wave UVA (320–400 nm). However, UV radiation in the wavelength range of 100–200 nm might not propagate in the air, while UV light in the wavelength range of 200–400 nm might have an impact on human health.[1] The skin is the largest organ of the human body, and it effectively assists the body in resisting external damage. In recent decades, there has been a decrease in global ozone, resulting in the gradual thinning of the atmospheric ozone layer, and enhancement of the ground UV radiation, and especially an increase in the UVB band content.[2] UVB radiation has a strong destructive effect on organisms, and the damage of UVB to the skin is 800–1000 times stronger as compared to the effect of an identical dose of UVA.[3] Therefore, in order to seek safe and effective sun protection measures for the skin, the development of natural antioxidants is of great significance for preventing skin damage caused by UV rays.

Lemons are evergreen citrus trees that belong to the Rutaceae family. As a high-yield crop, lemons are widely used as a fruit and are also processed into fruit juice, jam, and other foods.[4] Because lemon peels are thick and rough, they are not widely used in traditional processing applications. There are abundant amounts of lemon trees in China, with uric lemons currently being the main variety planted in Guangxi, Guangdong, Sichuan, and Yunnan provinces. Among them, the yield of lemons cultivated in Sichuan is the largest.[5] Lemon fruit is rich in nutrients, and contains other active ingredients including supplementary fiber, multi-vitamins, flavonoids, phenolic derivatives, limonin, and minerals.[6,7] The active ingredients in lemon fruit effectively lower blood sugar and blood lipids, prevent vascular hyperplasia, and exert anti-inflammatory, anti-tumor, anti-oxidation, anti-virus, and anti-osteoporosis effects.[8–10] Lemon peels are mostly discarded during processing, and are only used in traditional Chinese medicine for strengthening the spleen.[11]

The flavonoids in lemons effectively remove free radicals such as hydrogen peroxide and superoxide anions. Different parts of the lemon contains different amounts of flavonoids, and the types are also different. According to related research, the primary flavonoids in lemon fruit are rutin, hesperidin, and

[a]*National Citrus Engineering Research Center, Chongqing 410125, China. E-mail: liguijie@cric.cn; Tel: +86-23-6297-5381*

[b]*Citrus Research Institute, Southwest University, Chongqing 400712, China*

[c]*Guang'an Zhengwang Agriculture Co., Ltd, Guang'an 638000, Sichuan, China*

[d]*Chongqing Collaborative Innovation Center for Functional Food, Chongqing University of Education, Chongqing 400067, China*

sage citrin, which comprise more than 90% of the total flavonoids in lemon fruit,[12] although lemon peels also contained other flavonoids.[13] Studies have shown that flavonoids from plants effectively prevent photodamage caused by UV rays by inhibiting inflammation, oxidative stress, and DNA damage, and preventing any imbalance in the synthesis and degradation of the extracellular matrix.[12,13]

In this study, the total flavonoids extracted from lemon peels were studied. Lemon peel flavonoid extract was applied to the posterior skin of mice after construction of a mouse skin damage model induced by UVB. Then, the serum and skin tissue of the mice were observed by biochemical and molecular biological methods so as to identify the interventional effect of lemon peel flavonoids on UVB-induced skin damage in mice, and the mechanism of action of lemon peel flavonoids was studied.

2 Materials and methods

2.1 Extraction of flavonoids from lemon peels

After fresh lemons were cleaned, the skin was peeled, and then, the lemon peels were freeze-dried and crushed into a fine powder. For extraction, 50 g of fine powder was mixed with 70% ethanol according to the ratio of 15 : 1, and subject to ultrasonication for 10 min at 60 °C. After the process was completed, the mixture was warmed in a water bath at 60 °C for 2 h. Then, a suction filtration device was used to remove the ethanol, and the filter residue was then extracted multiple times. The resulting filtrate was distilled with a rotary evaporator, and the ethanol was recovered at the same time. Lastly, the resulting concentrated liquid was freeze-dried for 4 h, and the final dried powder consisted of the total flavonoids from lemon peels.[14]

2.2 Composition analysis of lemon peel flavonoids (LPF)

The components of LPF were analyzed by HPLC-DAD (quaternary gradient pump, DAD detector), the liquid chromatography conditions were Accucore-C_{18} column (2.6 μm, 4.6 mm × 150 mm), mobile phase A: 0.5% acetic acid aqueous solution, mobile phase B: 100% acetonitrile, column temperature: 30 °C, flow rate: 0.5 mL min^{-1}, detection wavelength: 285 nm, injection volume: 10 μL, chromatographic running time: 40 min. The gradient elution conditions of mobile phase were shown in Table 1.

Table 1 Gradient elution conditions of mobile phase[a]

Time (min)	Current speed (mL min^{-1})	% A	% B
0	0.5	88.0	12.0
30	0.5	55.0	45.0
35	0.5	0.0	100.0
40	0.5	0.0	100.0

[a] A: 0.5% acetic acid aqueous solution, mobile phase B: 100% acetonitrile.

2.3 Construction of UVB radiation mouse skin injury model and group administration

Seven-week-old male Kunming mice (Chongqing Medical University, Chongqing, China) were used in all experiments. The long hair on the backs of the mice was cut off with scissors, and any remaining hair was then gently scraped off with a hair removal knife. A hair removal solution was then applied to the same area on the backs of the mice to completely remove any remaining hair. The hair removal area was 2 cm × 2 cm, and hair removal was performed every other day. A UV light box was constructed using four 313 nm UVB lamps, and the irradiation height was adjusted to 20 cm. The mice were randomly divided into 5 groups: normal group (Normal), model group (Model), group treated with topical application of vitamin C (VC), group treated with topical application of low concentration of lemon peel flavonoid (LPFL), and group treated with topical application of high concentration of lemon peel flavonoid (LPFH). All of the mice were given access to food and drinking water ad libitum every day. The normal group received no treatment; the model group was treated with 2 h of UV irradiation per day; 5% VC (vehicle control) was applied to the hair removal area of the VC group mice every day, who were then placed under UV light for 2 h after 0.5 h; the LPFL and LPFH group mice were treated with topical application of 2.5% and 5% LPF, respectively, on their hair removal sites, and subsequently placed under ultraviolet light for 2 h after 0.5 h; and this process lasted 4 weeks.[15] After the experiment, retro-orbital sinus blood collection was performed. After the mice were euthanized, the bare skin at the hair removal site was removed for later use. All animal procedures were performed in accordance with the Guidelines for Care and Use of Laboratory Animals of Chongqing University of Education and approved by the Animal Ethics Committee of Chongqing Collaborative Innovation Center for Functional Food, Chongqing University of Education (202004005B).

2.4 Determination of serum oxidation index

The mouse blood was centrifuged at 3220 × *g* for 10 min at 4 °C. The supernatant was removed to prepare serum, the 50 μL of serum samples were processed according to the corresponding malondialdehyde (MDA), catalase (CAT), superoxide dismutase (SOD), (Nanjing Jiancheng Bioengineering Institute, Nanjing, Jiangsu, China) and 8-iso-PGF2a (Shanghai Shiruike Biotechnology Co., Ltd, Shanghai, China) detection kit instructions, and their levels were determined at the absorbance of 532, 240, 450 and 450 nm.

2.5 Determination of serum inflammation enzyme-linked immunosorbent assay (ELISA) index

After the serum oxidation index was measured, the serum samples were processed according to the instructions of the corresponding IL-1β, IL-6, IL-10, and TNF-α detection kits (Abcam, Cambridge, Massachusetts, USA), and their levels were determined.

2.6 Pathological observation of the skin

The removed bare skin was cut into squares with a size of approximately 0.5 cm^2, fixed in 10% formalin solution, stained with hematoxylin and eosin (H&E) and Masson, and then observed and photographed with a microscope (BX43 microscope, Olympus, Tokyo, Japan).

2.7 qPCR

First, 100 mg of mouse skin tissue was placed in a homogenate tube, 1 mL TRIzol reagent (all qPCR experimental reagents and consumables came from Thermo Fisher Scientific, Inc., Waltham, MA, USA) and 5 steel balls were added, and the mixture was homogenized in a tissue homogenizer. Then, the tissue homogenate was added to a centrifuge tube, chloroform was added, and the RNA supernatant was obtained by freeze centrifugation. Isopropanol solution was then added for refrigerated centrifugation, and the supernatant was removed to obtain a yellow-white RNA precipitate. A 75% ethanol solution prepared with RNase-free water was added to the RNA precipitate, which was washed by shaking up and down, and lastly, refrigerated centrifugation was performed again. A 75% ethanol solution prepared by filtering with diethyl pyrocarbonate (DEPC) water was added to the resulting RNA precipitate, which was shaken up and down for washing. Then, after refrigerated centrifugation, the upper tube was discarded, and chloroform was added. The supernatant RNA was obtained by refrigerated centrifugation, which was repeated once more after the addition of isopropanol solution, and a yellow and white RNA precipitate was then obtained after removing the supernatant. Once again, a 75% ethanol solution prepared with RNase-free water was added to the RNA precipitate, which was then shaken up and down for washing, and lastly, refrigerated centrifugation was performed again. With purification complete, 1 μL of RNA was mixed with 49 μL of DEPC water in a polyethylene tube, and this solution was used to measure the RNA concentration with a micro-spectrophotometer.

For qPCR, 1 μL of a 1 μg μL^{-1} RNA solution, 1 μL of Oligo dT, and 10 μL of sterile ultrapure water were mixed and then equilibrated by heating at 65 °C in a PCR instrument for 5 min. Next, 4 μL of 5× reaction buffer, 1 μL of Ribolock RNase Inhibitor (20 U mL^{-1}), and 2 μL of 100 mM dNTP Mix were added, and the solution was mixed well. Then, 7 mL of each sample and 1 μL of Revert Aid M-mu/N RT were then added. The RNA was reverse (Table 2) transcribed into cDNA at 42 °C for 60 min and 70 °C for 5 min. Using GAPDH as an internal reference, the expression level of mRNA expressed in the liver was detected by the RT-qPCR instrument.[16]

2.8 Data processing and analysis

SPSS 18.0 software was used for data analysis and processing, and the results are displayed in the form of the mean ± standard deviation. The data for each group were compared by single factor analysis of variance (ANOVA), and significant difference was defined at $P < 0.05$.

Table 2 Sequences of the primers used for the mice skin tissue

Gene name	Sequence
SOD1 (Cu/Zn–SOD)	Forward: 5′-AACCAGTTGTGTTGTCAGGAC-3′
	Reverse: 5′-CCACCATGTTTCTTAGAGTGAGG-3′
SOD2 (Mn–SOD)	Forward: 5′-CAGACCTGCCTTACGACTATGG-3′
	Reverse: 5′-CTCGGTGGCGTTGAGATTGTT-3′
CAT	Forward: 5′-GGAGGCGGGAACCCAATAG-3′
	Reverse: 5′-GTGTGCCATCTCGTCAGTGAA-3′
Nrf2	Forward: 5′-CAGTGCTCCTATGCGTGAA-3′
	Reverse: 5′-GCGGCTTGAATGTTTGTC-3′
HO-1	Forward: 5′-ACAGATGGCGTCACTTCG-3′
	Reverse: 5′-TGAGGACCCACTGGAGGA-3′
NF-κB	Forward: 5′-GAGGCACGAGGCTCCTTTTCT-3′
	Reverse: 5′-GTAGCTGCATGGAGACTCGAACA-3′
IκB-α	Forward: 5′-TGAAGGACGAGGAGTACGAGC-3′
	Reverse: 5′-TGCAGGAACGAGTCTCCGT-3′
p38 MAPK	Forward: 5′-GATACAAAGACGGGGCATCG-3′
	Reverse: 5′-CACGATGTTGTTCAGGTCCG-3′
COX-2	Forward: 5′-GGTGCCTGGTCTGATGATG-3′
	Reverse: 5′-TGCTGGTTTGGAATAGTTGCT-3′
GAPDH	Forward: 5′-AGGTCGGTGTGAACGGATTTG-3′
	Reverse: 5′-GGGGTCGTTGATGGCAACA-3′

3 Results

3.1 Composition of lemon peel flavonoids (LPF)

It can be seen from Fig. 1 that the flavonoids in lemon peel are isomangiferin, rutin, astragalin, naringin and quercetin, with the contents of 327.17 mg g^{-1}, 179.52 mg g^{-1}, 38.91 mg g^{-1}, 12.66 mg g^{-1} and 3.78 mg g^{-1} respectively. The content of isomangiferin is higher, followed by rutin.

3.2 Effects of LPF on MDA, CAT, SOD, and 8-iso-PGF2a levels in the serum of UVB-irradiated mice

Compared with the normal group, there was a significant increase in the serum MDA of the model group mice ($P < 0.05$), and SOD and CAT significantly decreased ($P < 0.05$), proving the successful establishment of the skin damage model (Table 3). Compared with the model group, the serum MDA and 8-iso-PGF2a of the flavonoid-treated group and the VC-treated group significantly decreased ($P < 0.05$), while SOD and CAT significantly increased ($P < 0.05$). The serum MDA, CAT, SOD, and 8-iso-PGF2a levels of mice treated with LPFH were closer to those of the normal group than those of the other groups.

3.3 Effect of LPF on the level of inflammatory factors in the serum of UVB-irradiated mice

Compared with the normal group, the serum levels of IL-1β, IL-6, IL-I0, and TNF-α in the model group mice were significantly increased ($P < 0.05$, Table 4). Compared with the model group, the IL-1β, IL-6, IL-10, and TNF-α serum levels of the mice in the flavonoid- and VC-treated groups were significantly decreased ($P < 0.05$). At the same application concentration, LPFH more strongly downregulated the levels of IL-1β, IL-6, IL-10, and TNF-α in the serum as compared to VC.

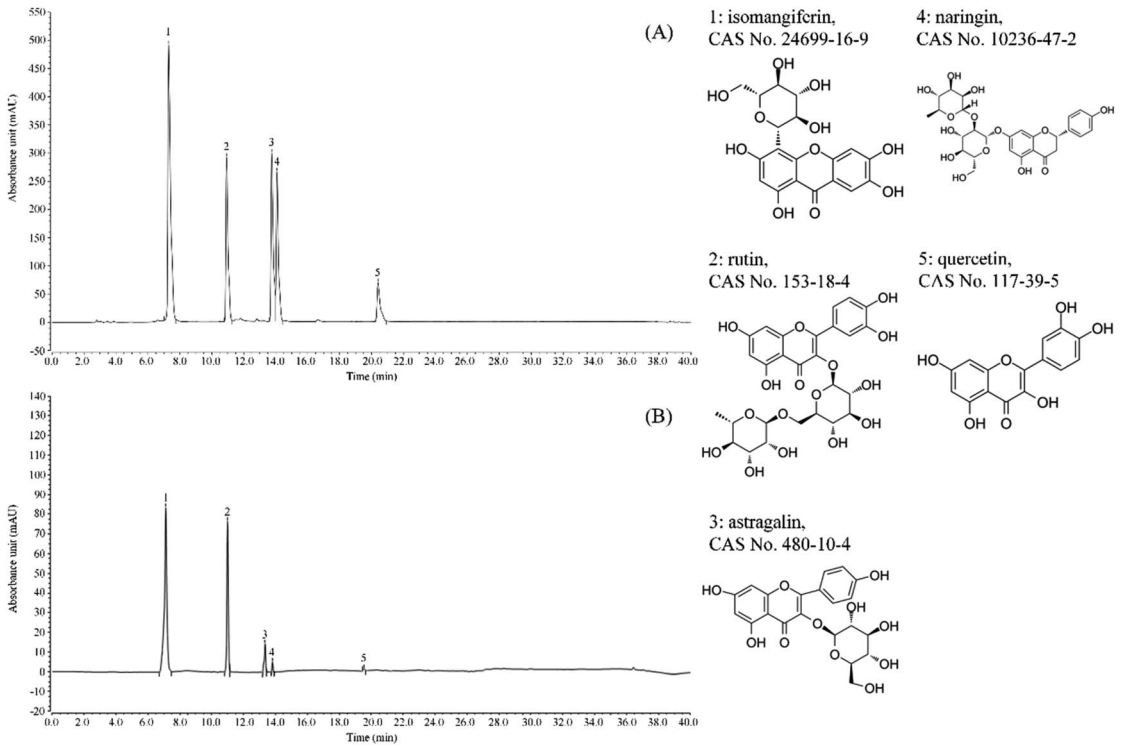

Fig. 1 Flavonoids constituents of lemon peel. (A) Standard chromatograms; (B) lemon peel flavonoids chromatograms. 1: isomangiferin; 2: rutin; 3: astragalin; 4: naringin; 5: quercetin.

3.4 Pathological observation of mouse skin tissue

H&E staining of pathological sections revealed that the skin tissue of the normal group exhibited a clear cell structure, the epidermal layer was intact, the dermis layer was thin, and the fibers covering it were neatly distributed (Fig. 2). After the model group was exposed to ultraviolet rays, the epidermal structure of the mouse skin tissue was incomplete, the thickness of the epidermal layer significantly increased, the dermis layer showed disordered tissues and deformed fibers, and a large number of inflammatory cells infiltrated, indicating that the skin damage model was successfully established. In the VC-treated group, the epidermal structure of the skin tissue of the mice was relatively complete, the dermal layer tissue was neatly arranged, and the inflammatory cells of the dermal layer were significantly reduced. Compared with the model group, the epidermal thickening of the skin tissue of mice in the LPFL-treated group was reduced, and there was decreased disorder of the dermal tissue arrangement. Compared with the model group, the morphological changes of the skin tissue of the mice in the LPFH-treated group were significantly improved, and closely resembled that of the normal group. The epidermal structure was complete, and the dermis layer was neatly arranged.

Masson staining of pathological sections showed that collagen fibers in the normal group were darker, and were arranged in an orderly and evenly distributed manner (Fig. 3). There was a small amount of lightly stained collagen fibers in the skin tissue of the model group mice. The collagen fibers in the superficial layer of the dermis exhibited the most obvious

Table 3 Levels of SOD, CAT, MDA, and 8-iso-PGF2a in serum of mouse[a]

Group	SOD (U mL^{-1})	CAT (U mL^{-1})	MDA (μmol L^{-1})	8-Iso-PGF2a (pg mL^{-1})
Normal	51.74 ± 1.81^{a}	10.87 ± 0.22^{a}	8.71 ± 0.80^{e}	163.57 ± 18.92^{e}
Model	36.60 ± 0.80^{e}	38.25 ± 2.41^{e}	21.19 ± 0.85^{a}	408.23 ± 21.49^{a}
VC	43.90 ± 2.00^{c}	24.99 ± 0.79^{c}	15.48 ± 0.91^{c}	279.62 ± 19.32^{c}
LPFL	40.22 ± 1.06^{d}	18.87 ± 0.98^{d}	18.36 ± 0.81^{b}	225.67 ± 14.85^{b}
LPFH	47.21 ± 1.98^{b}	33.16 ± 1.68^{b}	11.19 ± 0.40^{d}	349.71 ± 22.50^{d}

[a] "±" for standard deviation ($N = 10$/group). [a–e]Using Tukey's honestly significantly different test, there was no significant difference between the two groups with the same superscript ($P > 0.05$), and there is significant difference between the two groups with different superscript ($p < 0.05$). VC: mouse was applied with 5% vitamin C; LPFL: mouse was applied with 2.5% lemon peel flavonoids; LPFH: mouse was applied with 5% lemon peel flavonoids.

Table 4 Serum levels of IL-6, IL-10, TNF-α, and IL-1β in mice[a]

Group	IL-6 (pg mL^{-1})	IL-10 (pg mL^{-1})	TNF-α (pg mL^{-1})	IL-1β (pg mL^{-1})
Normal	46.56 ± 1.12[e]	238.42 ± 28.32[e]	253.04 ± 33.12[e]	34.00 ± 1.27[e]
Model	106.46 ± 3.97[a]	776.32 ± 45.71[a]	566.96 ± 16.07[a]	146.00 ± 13.03[a]
VC	67.24 ± 2.58[c]	581.58 ± 36.59[c]	377.30 ± 21.78[c]	80.17 ± 3.96[c]
LPFL	88.43 ± 2.60[b]	656.84 ± 26.97[b]	454.96 ± 37.74[b]	106.17 ± 6.80[b]
LPFH	57.21 ± 1.70[d]	464.74 ± 20.08[d]	310.87 ± 25.92[d]	62.17 ± 4.43[d]

[a] "±" for standard deviation ($N = 10$/group). [a–e]Using Tukey's honestly significantly different test, there was no significant difference between the two groups with the same superscript ($P > 0.05$), and there is significant difference between the two groups with different superscript ($p < 0.05$). VC: mouse was applied with 5% vitamin C; LPFL: mouse was applied with 2.5% lemon peel flavonoids; LPFH: mouse was applied with 5% lemon peel flavonoids.

changes, with fractures, reduced numbers, varying thickness, and disordered arrangement. At the same concentration, there was less damage to the dermal collagen fibers in the skin tissue of the mice in the VC-treated group as compared with the model group, the collagen fiber staining was lighter, and the number was reduced. Compared with the model group, there was a significant improvement in the changes in the collagen fibers in the skin tissue of the mice in the LPF-treated group, the degree of collagen fiber damage was reduced, and the arrangement was relatively neat.

3.5 Effect of LPF on the mRNA expression of *SOD1*, *SOD2*, *CAT*, *Nrf2*, and *HO-1* in mouse skin

The experimental results showed that the expression of *SOD1*, *SOD2*, *CAT*, *Nrf2*, and *HO-1* in the skin of the normal group mice was the strongest (Fig. 4), while that in the model group was the weakest. The application of VC, LPFL, and LPFH significantly ($P < 0.05$) upregulated the expression of *SOD1*, *SOD2*, *CAT*, *Nrf2*, and *HO-1* in the skin of UVB-induced skin-damaged mice, and LPFH exhibited the strongest upregulation ability.

3.6 Effect of LPF on the mRNA expression of *NF-κB*, *IκB-α*, *p38 MAPK*, and *COX-2* in mouse skin

Fig. 5 shows that compared with the normal group mice, the expression of *NF-κB*, *p38 MAPK*, and *COX-2* in the skin of mice with UVB-induced skin damage increased, while the expression of *IκB-α* decreased. Both VC and LPF application decreased the expression of *NF-κB*, *p38 MAPK*, *COX-2* and enhanced the expression of *IκB-α* in mice with skin injury, and the effect of LPFH was stronger than that of VC and LPFL.

4 Discussion

Excessive exposure to ultraviolet rays can cause acute skin inflammation, which manifests as erythema, edema, hyperplasia, and burning and tingling in the skin of the exposed area, which might cause blisters and erosion in severe cases, and might be followed by peeling and pigmentation after inflammation.[17] Because UVB mainly acts on the chromophores in the epidermis, the histopathological manifestation of acute inflammation is obvious keratinization, apoptosis, and edema. In severe cases, it can affect the full layer of the epidermis, and

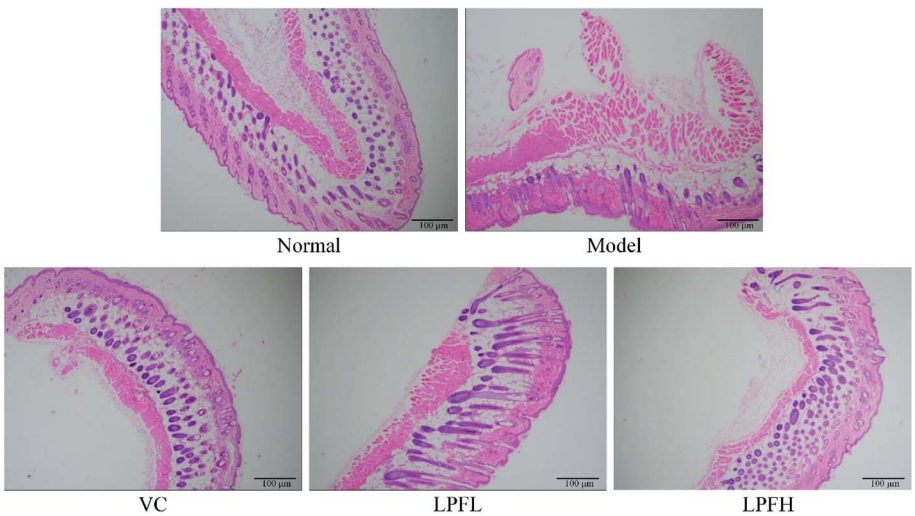

Fig. 2 Hematoxylin and eosin (H&E) pathological observations of skin tissues from mice. Magnification 100×. VC: mouse was applied with 5% vitamin C; LPFL: mouse was applied with 2.5% lemon peel flavonoids; LPFH: mouse was applied with 5% lemon peel flavonoids.

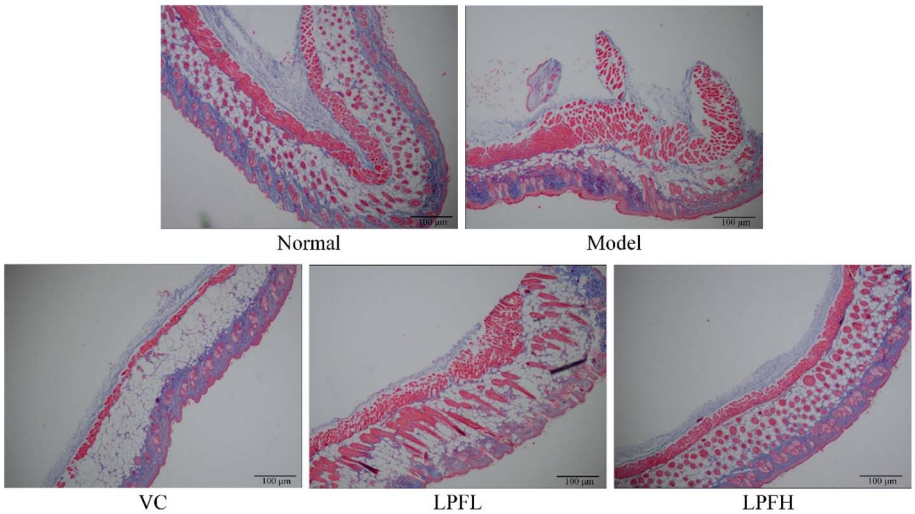

Fig. 3 Masson pathological observations of skin tissues from mice. Magnification 100×. VC: mouse was applied with 5% vitamin C; LPFL: mouse was applied with 2.5% lemon peel flavonoids; LPFH: mouse was applied with 5% lemon peel flavonoids.

be accompanied by neutrophil accumulation in the epidermis, dermal telangiectasia, and infiltration of lymphatic tissue cells around the blood vessels.[18]

During the experiment, the mice were irradiated with UVB for 4 weeks, which clearly demonstrated continuous skin damage sustained by UVB, and simulated the damaging effect of UVB on the skin in an objective and specific manner. After successfully establishing a damaged skin mouse model, the skin at the hair removal area on the backs of the mice was stained with H&E and Masson for later observation. UVB radiation causes many changes such as damage to the skin's epidermal structure, rupture of collagen fibers, and accompanying infiltration of inflammatory cells. After UVB radiation, epidermal keratinocytes release a large amount of inflammatory mediators and chemokines, such as IL-1, IL-6, IL-10, and TNF-α, and inflammatory cell hyperplasia occurs in the later stage of inflammation.[19] Previous studies have shown that the application of flavonoids effectively decreases the occurrence of UVB-induced skin inflammation, and in this study, similar results were obtained. The application of LPF decreases the epidermal inflammation in mice with UVB-induced skin damage.

The skin's own antioxidant system efficiently removes low levels of reactive oxygen species (ROS). However, excessive exposure to UVB causes large amounts of ROS to be produced, resulting in oxidative stress.[20] Excessive ROS can then cause damage to DNA, proteins, and lipids, and might eventually lead to cell apoptosis or even skin cancer.[21] Many studies have shown that flavonoids exert excellent antioxidant effects.[22–24] Most natural flavonoids exert anti-photosensitivity, anti-oxidation, and anti-inflammatory damage effects, and they prevent skin cell damage by removing free radicals in the skin.[25]

SOD is an active substance that protects beneficial free radicals and maintains their balance in living systems, thereby effectively blocking oxidative stress damage.[26] Therefore, SOD activity is an important indicator of anti-oxidation. In the current study, SOD activity in the LPF-treated groups significantly increased, indicating that LPF increased the SOD activity in mice. As an endogenous oxygen scavenger, CAT effectively prevents excessive cellular oxidation and decreases the oxidative damage in cells.[27] In our experiments, the CAT activity of the LPF-treated groups significantly increased, indicating that LPF effectively decreased the UV damage to the skin

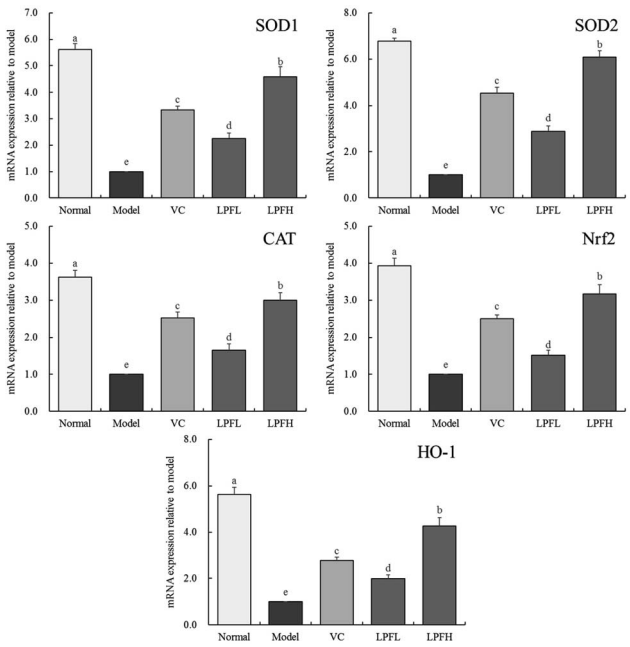

Fig. 4 SOD1, SOD2, CAT, Nrf2 and HO-1 mRNA expression of skin tissues in mice. "±" for standard deviation. $^{a-d}$Using Tukey's honestly significantly different test, there was no significant difference between the two groups with the same superscript ($P > 0.05$), and there is significant difference between the two groups with different superscript ($P < 0.05$). VC: mouse was applied with 5% vitamin C; LPFL: mouse was applied with 2.5% lemon peel flavonoids; LPFH: mouse was applied with 5% lemon peel flavonoids.

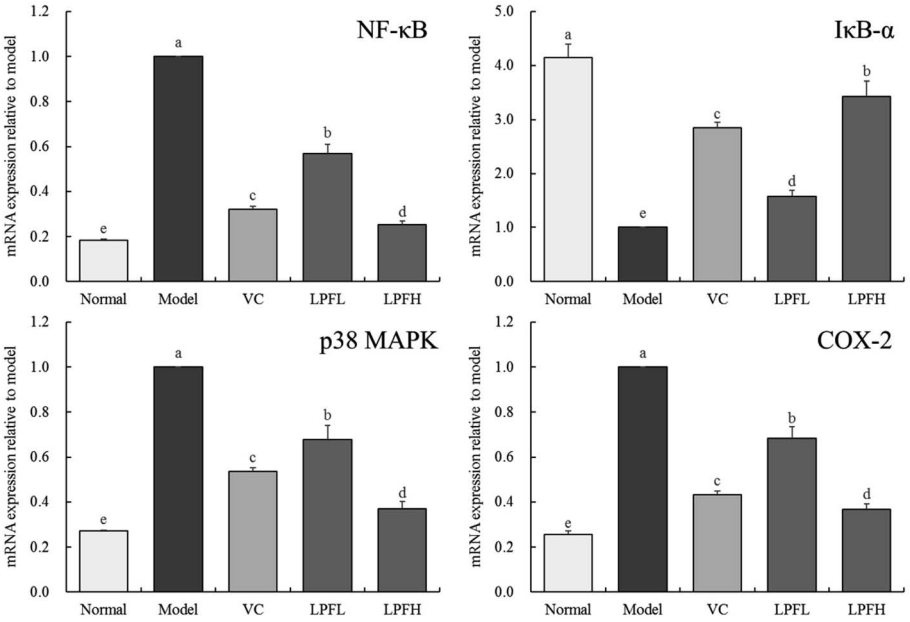

Fig. 5 NF-κB, IκB-α, p38 MAPK and COX-2 mRNA expression of skin tissues in mice. "±" for standard deviation. $^{a-d}$Using Tukey's honestly significantly different test, there was no significant difference between the two groups with the same superscript ($P > 0.05$), and there is significant difference between the two groups with different superscript ($P < 0.05$). VC: mouse was applied with 5% vitamin C; LPFL: mouse was applied with 2.5% lemon peel flavonoids; LPFH: mouse was applied with 5% lemon peel flavonoids.

of mice by increasing the CAT activity. MDA effectively reflects the degree of lipid affected by ROS in the body, and indirectly reflects the cell damage.[28] 8-Iso-PGF2a has strong polarity, and the amount of esterified 8-iso-PGF2a on cell membrane will increase after oxidative damage, which will damage the cell membrane, damage the structure and function of cells, and even lead to cell death.[29] Further studies also confirmed that 8-iso-PGF2a is only related to oxygen free radicals and can specifically reflect the degree of oxidative damage in human body.[30] In the current study, the levels of MDA and 8-iso-PGF2a in the model group were significantly higher than that in the normal group, while the levels of MDA and 8-iso-PGF2a in the LPF-treated group were significantly lower than that in the model group, indicating that a certain degree of antioxidant activity can be attributed to LPF.

Nrf2 is a key factor in cell defense against oxidative stress, and Nrf2 is also an essential regulator for inducing phase II enzyme gene expression. HO-1 in phase II enzymes had a protective effect upon cells, and it catalyzed heme to produce biliverdin, carbon monoxide, and iron. Biliverdin is transformed into bilirubin, while Nrf2 and HO-1 are powerful free radical scavengers in the body.[17] The flavonoids applied to the skin of hairless mice increased the expression of Nrf2 mRNA, and the Nrf2 transferred to the nucleus then combined with antioxidant response elements to subsequently induce HO-1 mRNA expression and exert antioxidant effects.[31] Additionally, flavonoid treatment of HaCaT cells irradiated with UVB resulted in an increase in the expression of intracellular antioxidants HO-1 and NQO1 by promoting the transfer of Nrf2 into the nucleus, thereby demonstrating excellent antioxidant activity.[32] Oxidative stress is related to Nrf2-HO-1-ROS pathway. By regulating Nrf2-HO-1-ROS pathway, the damage degree of oxidative stress can be reduced, so as to reduce inflammation.[33] In this study, LPF could protect skin by regulating Nrf2/HO-1 signaling pathway.

COX-2, p38, NF-κB, and I-κB are all important factors related to inflammation.[17] The change of Bcl-2 expression is related to the level of IL-1β, and can also affect the expression of p38. The regulation of Bcl-2 expression can control multiple signal pathways to reduce cell damage.[34,35] The flavonoids acting on human keratinocytes HaCaT inhibit the production of UVB-induced COX-2 by inhibiting the p38 MAPK signaling pathway.[36] By applying flavonoids to the back of SKH-1 hairless mice, it was found that it could suppress the levels of inflammatory cytokines TNF-α, IL-1β, and IL-6 through inhibiting the phosphatidylinositol 3-kinase (PI3K)/protein kinase B (Akt)/NF-κB pathways, and decrease the expression of COX-2, thereby decreasing PGE-2 and inhibiting UVB-induced inflammation.[37] UVB can cause oxidative damage to the cultured cells *in vitro*. Activation of PPAR-γ can promote the expression of COX-2 and the production of PGE2, thus protecting the cells.[38] Flavonoids also interfere with Hs68 fibroblasts exposed to ultraviolet radiation. Flavonoids enhance the expression of NF-κB inhibitors (I-κB) by inhibiting the activation of MAPK, thereby inhibiting NF-κB translocation into the nucleus, synergistically decreasing the level of p-CREB Ser-133 in the PI3K/Akt/cAMP response element-binding protein (CREB) pathway, and decreasing the activation of NF-κB so as to achieve the inhibition of COX-2, thereby decreasing the level of PGE-2 and thus alleviating any UV-induced inflammatory response.[39] The application of flavonoids to HaCaT cells indicates that it interferes with or directly inhibits the p38 MAPK pathway by decreasing the generation of

ROS to subsequently inhibit the release of UVB-induced proinflammatory mediators such as IL-6, TNF-α, PGE-2, and COX-2.[40] Chinese patent medicine of natural plants can reduce the level of MDA and enhance the activity of SOD, so as to weaken the activation of NF-κB pathway, reduce visceral damage and protect the body,[41] LPF also played a similar role in this study. Meanwhile, LPF regulated the expression of COX-2, p38 MAPK, NF-κB, and IκB-α in UVB-damaged mouse skin so that it normalized. Thus, IPF plays a role in interfering with UVB-induced skin damage.

HPLC is a common experimental method which can accurately determine the effective components of plants, and can be verified accurately in both component identification and fingerprint identification.[42] Therefore, this method is also used to identify the components of samples in this study. From HPLC assay, isomangiferin, rutin, astragalin, naringin, and quercetin are the main flavonoids present in LPF. Isomangiferin is an antioxidant flavonoid with antitussive, expectorant, cardiotonic, diuretic, and antidepressant effects. *In vivo* animal studies also showed that it could repair liver damage caused by high-fat feed.[43] Studies showed that applying rutin on the backs of hairless mice before UVB radiation attenuated the UVB-induced phosphorylation of p38 MAPK and c-Jun-N-terminal kinase (JNK) by inhibiting the formation of ROS, thereby inhibiting DNA binding in mouse skin that activated activator protein-1 (AP-1); it also inhibited the phosphorylation of transcription activator-3. These two actions synergistically inhibited the expression of COX-2 and iNOS in skin treated with UVB.[44] Applying rutin to the backs of hairless mice exposed to UVB decreased the production of UVB-induced ROS and lipid peroxide.[45] Astragalin is a natural flavonoid compound widely present in medicinal plants. It has anti-inflammatory, antioxidant, cardiotonic, anti-arrhythmia, analgesic, antibacterial, anti-allergic, and anti-hepatotoxic effects as well as the effects of enhancing immune resistance, stimulating the production of interferon, dilating blood vessels, and protecting the myocardium.[46] Naringin exhibits anti-inflammatory, anti-viral, anti-cancer, anti-mutation, anti-allergy, anti-ulcer, analgesic, and blood pressure-lowering effects. Naringin also lowers blood cholesterol, decreases the formation of thrombus, and increases the local microcirculation and nutrition supply, thereby indicating that it could be used to produce drugs for preventing and treating cardiovascular and cerebrovascular diseases.[47] Quercetin decreases intracellular ROS levels, which decreases DNA damage and also prevents cell membranes and mitochondria from being attacked by ROS. Additionally, quercetin blocked the inhibition of cell membrane fluidity reduction and mitochondrial membrane depolarization, thereby blocking the inhibition of the outflow of cytochrome *c*, which in turn could inhibit apoptosis.[48] Previous studies have shown that due to the chemical structure and microbial action factors among the active substances, synergistic effects may also occur, thus enhancing the efficacy.[49] The protective effect of LPF on the skin may mainly come from these 5 chemical substances, the mechanism of the relationship between these 5 active ingredients requires further study.

5 Conclusions

In this study, a UVB-induced animal skin damage model was established to verify that LPF effectively protected the skin. LPF interfered with the oxidative stress and inflammation in mouse skin caused by UVB, thereby decreasing the skin's oxidative damage and inflammation. Molecular biology experiments results confirmed that LPF enhanced antioxidant enzymes, such as SOD and CAT, regulated Nrf2/HO-1, increased the antioxidant capacity, and regulated the p38 MAPK signaling pathway to control inflammation through 5 main flavonoid compounds, thus playing a biological role in protecting the skin. However, our research was limited to the study of animals, and in future research, human experiments and deepening mechanism research will be needed.

Conflicts of interest

No conflicts of interest in this article.

Acknowledgements

This research was supported by Southwest University Office of University-local authorities cooperation project-Zhengwang agriculture high quality orchard construction and supporting technology research and development; Fundamental Research Funds for the Central Universities (XDJK2020C026), China.

References

1 T. Ohnaka, *Ann. Physiol. Anthropol.*, 1993, **12**, 1–10.
2 K. W. Chung, Y. J. Choi, M. H. Park, E. J. Jang, D. H. Kim, B. H. Park, B. P. Yu and H. Y. Chung, *J. Gerontol., Ser. A*, 2015, **70**, 959–968.
3 P. Zheng and L. H. Kligman, *J. Invest. Dermatol.*, 1993, **100**, 194–199.
4 K. L. Penniston, S. Y. Nakada, R. P. Holmes and D. G. Assimos, *J. Endourol.*, 2008, **22**, 567–570.
5 Y. Huang, X. L. Tu, X. L. Ma, J. Wang and X. L. Lv, *Sci. Technol. Food Ind.*, 2019, **40**, 83–88.
6 J. W. Zhang, L. Tan, Y. Z. Zhang, G. C. Zheng, Z. N. Xia, C. Z. Wan, L. D. Zhou, Q. H. Zhang and C. S. Yuan, *J. Chromatogr. B: Anal. Technol. Biomed. Life Sci.*, 2019, **1104**, 205–211.
7 P. G. Pifferi, I. Manenti, L. Morselli and G. Spagna, *Ital. J. Food Sci.*, 1993, **5**, 269–276.
8 H. M. Tag, O. E. Kelany, H. M. Tantawy and A. A. Fahmy, *J. Basic Appl. Zool.*, 2014, **67**, 149–157.
9 U. Vinitketkumnuen, R. Puatanachokchai, N. Lertprasertsuke, P. Kongtawelert, P. Picha and T. Matsushima, *Mutat. Res.*, 1996, **359**, 200–201.
10 D. Hamdan, M. Z. El-Readi, A. Tahrani, F. Herrmann, D. Kaufmann, N. Farrag, A. El-Shazly and M. Wink, *Z. Naturforsch., C: J. Biosci.*, 2011, **66**, 385–393.
11 F. Li and L. X. Liu, *World Latest Medicine Information*, 2016, **86**, 42–43.

12 C. A. Ledesma-Escobar, F. Priego-Capote and M. D. L. de Castro, *PLoS One*, 2016, **11**, e0148056.
13 Y. Miyake, K. Yamamoto, Y. Morismitsu and T. Osawa, *J. Agric. Food Chem.*, 1997, **45**, 4619–4623.
14 L. Zhuo, Q. D. Jiang, S. Q. Yuan and M. Zou, *Guizhou Agric. Sci.*, 2013, **41**, 143–145.
15 R. K. Yi, J. Zhang, P. Sun, Y. Qian and X. Zhao, *Molecules*, 2019, **24**, 1016.
16 R. R. Wang, X. F. Zeng, B. H. Liu, R. K. Yi, X. R. Zhou, J. M. Mu and X. Zhao, *Food Funct.*, 2020, **11**, 2679.
17 J. Tanaka, S. J. Shan, N. Kasajima and H. Shimoda, *Food Sci. Technol. Res.*, 2007, **13**, 310–314.
18 C. L. Saw, M. T. Huang, Y. Liu, T. O. Khor, A. H. Conney and A. N. Kong, *Mol. Carcinog.*, 2010, **50**, 479–486.
19 Y. Kim, S. K. Lee, S. Bae, H. Kim, Y. Park, N. K. Chu, S. G. Kim, H. R. Kim, Y. I. Hwang, J. S. Kang and W. J. Lee, *Immunol. Lett.*, 2012, **149**, 110–118.
20 J. N. Ho, Y. H. Lee, J. S. Park, W. J. Jun, H. K. Kim, B. S. Hong, D. H. Shin and H. Y. Cho, *Biol. Pharm. Bull.*, 2005, **28**, 1244–1248.
21 A. Tresserra-Rimbau, R. M. Lamuela-Raventos and J. J. Moreno, *Biochem. Pharmacol.*, 2018, **156**, 186–195.
22 V. D'Amelia, R. Aversano, P. Chiaiese and D. Carputo, *Phytochem. Rev.*, 2018, **17**, 611–625.
23 L. Zhang, P. Liu, L. Li, Y. Huang, Y. Pu, X. Hou and L. Song, *Molecules*, 2019, **24**, 122.
24 O. Coskun, A. Ocakci, T. Bayraktaroglu and M. Kanter, *Tohoku J. Exp. Med.*, 2004, **203**, 145–154.
25 N. Ahmad, H. Gali, S. Javed and R. Agarwal, *Biochem. Biophys. Res. Commun.*, 1998, **247**, 294–301.
26 S. I. Choi, J. H. Lee, J. M. Kim, T. D. Jung, B. Y. Cho, S. H. Choi, D. W. Lee, J. Kim, J. Y. Kim and O. H. Lee, *Int. J. Mol. Sci.*, 2017, **18**, 1200.
27 S. E. Jeon, S. Choi-Kwon, K. A. Park, H. J. Lee, M. S. Park, J. H. Lee, S. B. Kwon and K. C. Park, *Photodermatol., Photoimmunol. Photomed.*, 2003, **19**, 235–241.
28 Z. Ghlissi, N. Sayari, R. Kallel, A. Bougatef and Z. Sahnoun, *Biomed. Pharmacother.*, 2016, **84**, 115–122.
29 M. J. Shin, J. H. Lee, Y. Jang, E. Park, J. Oh, J. H. Chung and N. Chung, *Metabolism*, 2006, **55**, 918–922.
30 M. T. Mitjavila, M. Fandos, J. Salas-Salvadó, M. I. Covas, S. Borrego, R. Estruch, R. Lamuela-Raventós, D. Corella, M. Á. Martínez-Gonzalez, J. M. Sánchez, M. Bulló, M. Fitó, C. Tormos, C. Cerdá, R. Casillas, J. J. Moreno, A. Iradi, C. Zaragoza, J. Chaves and G. T. Sáez, *Clin. Nutr.*, 2012, **32**, 172–178.
31 J. Johnson, P. Maher and A. Hanneken, *Invest. Ophthalmol. Visual Sci.*, 2009, **50**, 22398–22406.
32 R. Foresti, S. K. Bains, T. S. Pitchumony, L. E. de Castro Brás, F. Drago, J. L. Dubois-Randé, C. Bucolo and R. Motterlini, *Pharmacol. Res.*, 2013, **76**, 132–148.
33 K. F. Zhai, H. Duan, G. J. Khan, H. Xu, F. K. Han, W. G. Cao, G. Z. Gao, L. L. Shan and Z. J. Wei, *J. Agric. Food Chem.*, 2018, **66**, 6073–6082.
34 K. F. Zhai, H. Duan, Y. Chen, G. J. Khan, W. G. Cao, G. Z. Gao, L. L. Shan and Z. J. Wei, *Food Funct.*, 2018, **9**, 2070–2079.
35 K. F. Zhai, H. Duan, C. Y. Cui, Y. Y. Cao, J. L. Si, H. J. Yang, Y. C. Wang, W. G. Cao, G. Z. Gao and Z. J. Wei, *J. Agric. Food Chem.*, 2019, **67**, 2856–2864.
36 J. W. Cho, K. Park, G. R. Kweon, B. C. Jang, W. K. Baek, M. H. Suh, C. W. Kim, K. S. Lee and S. I. Suh, *Exp. Mol. Med.*, 2005, **30**, 186–192.
37 H. C. Pal, M. Athar, C. A. Elmets and F. Afaq, *Photochem. Photobiol.*, 2015, **91**, 225–234.
38 N. Yoshizaki, T. Fujii, H. Masaki, T. Okubo, K. Shimada and R. Hashizume, *Exp. Dermatol.*, 2014, (S1), 18–22.
39 S. Gupta and H. Mukhtar, *Cancer Metastasis Rev.*, 2002, **21**, 363–380.
40 N. Yoshizaki, T. Fujii, H. Masaki, T. Okubo, K. Shimada and R. Hashizume, *Exp. Dermatol.*, 2014, **23**, 18–22.
41 K. F. Zhai, H. Duan, W. G. Cao, G. Z. Gao, L. L. Shan, X. M. Fang and L. Zhao, *J. Pharm. Sci.*, 2016, **130**, 94–100.
42 H. Duan, Z. Dong, H. Li, W. R. Li, S. X. Shi, Q. Wang, W. G. Cao, X. M. Fang, A. D. Fang and K. F. Zhai, *Food Chem. Toxicol.*, 2019, **134**, 110831.
43 B. Wang, J. Shen, Z. Wang, J. Liu, Z. Ning and M. Hu, *J. Breast Cancer*, 2018, **21**, 11–20.
44 K. S. Choi, J. K. Kundu, K. S. Chun, H. K. Na and Y. J. Surh, *Arch. Biochem. Biophys.*, 2014, **559**, 38–45.
45 A. Gęgotek, P. Rybałtowska-Kawałko and E. Skrzydlewska, *Oxid. Med. Cell. Longevity*, 2017, **2017**, 4721352.
46 O. H. You, E. A. Shin, H. Lee, J. H. Kim, D. Y. Sim, J. H. Kim, Y. Kim, J. H. Khil, N. I. Baek and S. H. Kim, *Phytother. Res.*, 2017, **31**, 1614–1620.
47 M. Jain and H. S. Parmar, *Inflammation Res.*, 2010, **60**, 483–491.
48 A. Murakami, H. Ashida and J. Terao, *Cancer Lett.*, 2008, **269**, 315–325.
49 R. K. Yi, F. B. Wang, F. Tan, X. Y. Long, Y. N. Pan and X. Zhao, *RSC Adv.*, 2020, **10**, 23510–23521.

